Progress In Electromagnetics Research Letters, Vol. 26, 105–114, 2011

A COMPACT FRACTAL DIPOLE ANTENNA FOR 915 MHz AND 2.4 GHz RFID TAG APPLICATIONS

H. Kimouche* **and H. Zemmour**

Microwaves and Radar Laboratory, Ecole Militaire Polytechnique, Bordj El Bahri, Algeria

Abstract—A compact printed dipole antenna using fractal shape for Radio Frequency IDentification (RFID) is presented. The proposed antenna consists of a third iteration fractal tree structure with the aim of reducing the antenna size. It occupies a volume of $78 \times 30 \times 1.58\,\mathrm{mm}^3$ and the radiator is composed of two arms. The antenna has been designed and optimized to cover the bi-band for passive RFID tag at 915 MHz and 2.4 GHz. A parametric study of the proposed antenna was carried out in order to optimize the main parameters. Details of the proposed antenna design and measurement results are presented and discussed.

1. INTRODUCTION

Radio Frequency IDentification (RFID) is an automatic identification method on storing and remotely retrieving data using devices called RFID tags or transponders. An RFID tag is a small object that can be attached to or incorporated into a product, animal or person. RFID tag contains an application-specific integrated circuit (ASIC) chip and an antenna to enable it to receive and respond to Radio-Frequency (RF) queries from RFID reader or interrogator. Passive tags require no internal power source, whereas active tags require a power source. Today most implantations involve passive technology for its low cost [1].

Several frequency bands have been standardized for this technology. Low-Frequency (LF, 125–134 KHz) and High-frequency (HF, 13.56 MHz) systems are the most mature and worldwide diffused technologies. Tags at these frequencies use inductive coupling between two coils in order to supply energy to the tag and send information.

Received 3 August 2011, Accepted 26 August 2011, Scheduled 2 September 2011

* Corresponding author: Hocine Kimouche (kimouche@ymail.com).

Ultra-High Frequency (UHF, 860–960 MHz) and microwave frequency (2.4 GHz and 5.8 GHz) systems use the technique of far field backscatter modulation.

Low-frequency (LF) and high-frequency (HF) active RFIDs operating with battery power and a moderate sized antenna can transmit over long distances. Thus, they can be used for livestock tracking, access control, point of sale, etc. Nonetheless, the biggest potential lies in ultra high-frequency (UHF) and microwave frequency. Passive RFIDs which operate without battery and a very small-size antenna can be used for item tracking, especially useful for global supply chain management. The challenge for this technology is to increase the read range and its flexibility to environment factors for different applications.

Several papers on passive RFID tags antennas design for dual band applications have appeared in the literature in recent years, the majority of these tags combining the HF and UHF frequency [2, 3] or UHF and microwave frequency [4–6]. For the characteristics of miniaturization, how to increase the efficiency of RFID tag antenna in the limited space becomes a crucial project in this technology and the fractal theory is a solution for this issue. Fractal theory was proposed by Mandelbrot in 1975 [7]. Fractal geometries have self-similarity and space-filling nature when applied to antenna design and can realize multi-frequency and size-reducing features [8]. Several fractal geometries have been explored for antennas with special characteristics such as Sierpinski monopole [9] Koch curves monopole [10] and tree monopole [11, 12]. They verified that fractal antenna has size-reducing feature within the limited space.

In this paper, a new small-size fractal shape tag antenna is proposed for RFID communications combining the UHF and microwaves bands. The antennas dimensions have been optimized in order to obtain operation in the US RFID UHF (902–928 MHz). Nevertheless, the tag can be tuned to operate in other UHF bands corresponding to the standards used in other countries (European: 865–868 MHz; Japan: 950–956 MHz).

2. ANTENNA CONFIGURATION

The configuration of the proposed antenna is shown in Figure 1. The dipole antenna mainly consists of two radiating arms with third iteration tree fractal shape and using an inductively coupled feeding rectangular loop. Each branch allows one of its ends to branch off in two directions with a branching angle of 60°, a branch length half of the previous and a trace width of 1 mm. In the next stage of iteration,

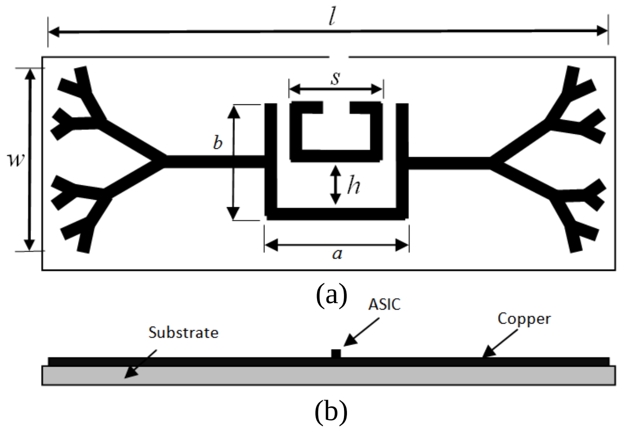

Figure 1. Geometry of the proposed antenna (a) Top view. (b) Cross-sectional view.

each of these branches is allowed to branch off again, by the same manner, and the process is continued until the third iteration. The dimensions of fractal tree branches and branching angle are taken so that the dipole without the rectangular loop is matched to the classical 50 Ω reference impedance port at 915 MHz. Therefore, the optimum length of the first branch is found to be 24 mm. The proposed antenna is printed on a low cost FR4 substrate with relative permittivity of 4.32 and thickness of 1.58 mm. The antenna dimensions are 78 mm × 30 mm ($l \times w$). It amounts to $0.23\lambda_0 \times 0.019\lambda_0$, where λ_0 is the wavelength in free space at the centre frequency of 915 MHz. The length of the conventional dipole antenna is about half the resonant wavelength and is 163.9 mm working at 915 MHz. The size of the proposed antenna without loop reduces about 37.2% comparing with conventional dipole antenna. Consequently, the structure of fractal shape is valid as a method of reducing the size of dipole.

The two ports at the center of the loop represent the location of the chip, and the feed is combined with the antenna body with mutual coupling. By suitably adjusting the loop length "s" and loop-radiating body spacing "h", the input impedance of the tag antenna can be complex conjugate to any desired microchip.

3. PARAMETRIC STUDY

The impedance matching between the antenna and the chip plays a crucial role in passive RFID tag design. The matching condition directly affects the maximum distance at which a RFID reader can detect the backscattered signal from tag. To ensure the inductive complex conjugate matching, an inductively coupled loop is used. The length "s" and spacing "h" of the added structure are the key geometric parameters to control the matching. A parametric study of the proposed antenna on these two parameters of the patch radiator has been optimized. Simulations are performed using commercially available software package such as Ansoft Designer.

3.1. The Effect of the Loop Length "s"

The loop length "s" is varied to obtain optimum reactance and resistance matching. As shown in Figure 2, the real and imaginary parts as a function of frequency were simulated for different lengths of "s" ($s = 10$, 12, and 12.5 mm). The other design parameters are $l = 78$ mm, $w = 30$ mm, $a = 17$ mm, $b = 13$ mm, $h = 1$ mm and a trace width of 1 mm. It is shown that the impedance of the antenna varies remarkably with the variation of the loop length s. For the proposed antenna, it can be noted that the loop length parameter influences the reactance of the input impedance of the tag antenna more strongly than the resistance, for both bands.

3.2. The Effect of the Loop-radiating Spacing "h"

The h parameter is the distance between the feeding loop and the antenna radiating body. As shown in Figure 3, the real and imaginary parts as a function of frequency were simulated for different spacing lengths of "h" ($h = 0.1$, 1, and 3 mm). The other design parameters are $l = 78$ mm, $w = 30$ mm, $a = 17$ mm, $b = 13$ mm and $s =$

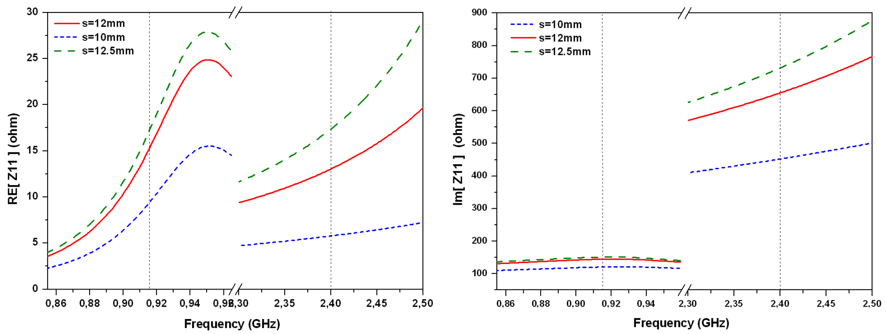

Figure 2. The effect of loop length "s".

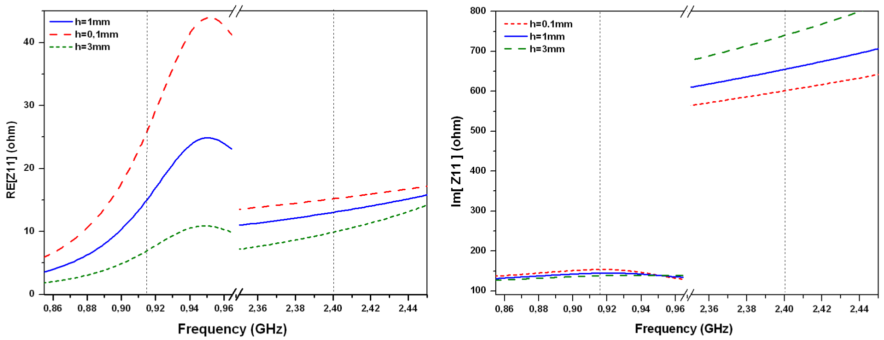

Figure 3. The effect of loop-radiating spacing "h".

12 mm. It is noticed that at 915 MHz, when the loop-radiating body spacing increases, both the resistance and reactance decrease but the resistance is more affected. While at 2.4 GHz, the resistance still nearly unchanged, and the reactance increases strongly.

For the proposed tag antenna, the combination of these geometric parameters allows the conjugate impedance matching of the tag antenna to a large variety of microchips which present a conjugate input impedance ($7 < R_{chip} < 26\,\Omega$) and ($110 < -X_{chip} < 151\,\Omega$) at 915 MHz; ($5 < R_{chip} < 17\,\Omega$) and ($450 < -X_{chip} < 740\,\Omega$) at 2.4 GHz.

4. EXPERIMENTAL RESULTS

The prototype of the proposed RFID dipole antenna with the optimal geometrical parameters was fabricated. Fractal antenna is optimized to be matched with a commercial tag (EPC GEN 2), which has input impedance of $(14 - \mathrm{j}144)\,\Omega$ at 915 MHz and $(14 - \mathrm{j}650)$ at 2.4 GHz. The measurement of the return loss and input impedance of the antenna were performed using an Agilent 8719ES Vector Network Analyzer (VNA). Since the geometry of the antenna is symmetrical and the simulations are performed using symmetrical boundary, the measurement setup is able to use the mirror method [13]. Half of the balanced dipole antenna on ground plane is one half of the balanced bow tie antenna shown. This unbalanced version of the bow tie antenna is soldered on a SMA connector, which is mounted on a ground plane. It should be noted that the VNA has been pre-calibrated without input SMA connector of the test structure, so we must shift the reference plane of the S matrix to the ground plane in order to eliminate the additional series impedance of the SMA connectors.

The Kurokawa method for calculating the power reflection coefficient is adapted to deal with the complex impedance of the tag antenna and the chip. This method describes a concept of power waves traveling back and forth between tag antenna and the chip by first introducing the following definitions for defining the return loss [14]:

$$\text{Return Loss} = S = 20\log\left(\left|\frac{Z_{ant} - Z_c^*}{Z_{ant} + Z_c}\right|\right) \tag{1}$$

Z_{ant} is related to the antenna impedance and Z_c is the chip impedance. In essence, this parameter shows what fraction of maximum power available from the chip is not delivered to the antenna. The maximum readable range "r" can then be calculated using the Friis free-space formula as [14]:

$$r = \frac{\lambda}{4\pi}\sqrt{\frac{P_t G_t G_r (1 - S)}{P_{th}}} \tag{2}$$

where λ is the wavelength, P_t is the power transmitted by the RFID reader, G_t is the gain of the transmitting antenna, $(P_t G_t)$ is the equivalent isotropic radiated power, G_r is the gain of the receiving tag antenna, and P_{th} is the minimum threshold power necessary to power up the chip.

4.1. Impedance Matching

Figure 4 shows the fabricated antenna, to ensure conjugate matching to the considered chip, the tag antenna optimization gives $l = 78$ mm, $w = 30$ mm, $s = 12$ mm, $a = 17$ mm, $b = 13$ mm and $h = 1$ mm.

The examined antenna performances are shown below.

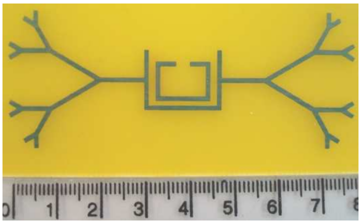

Figure 4. Photograph of the realized tag antenna.

The antenna's measured and simulated input impedances are shown in Figure 5. The measurements are performed using the Agilent HP8719ES vector network analyser and the mirror method. It is noticed, that the input impedance is roughly (16+j142) Ω at the frequency 915 MHz, and (18+j645) Ω at the frequency 2.4 GHz

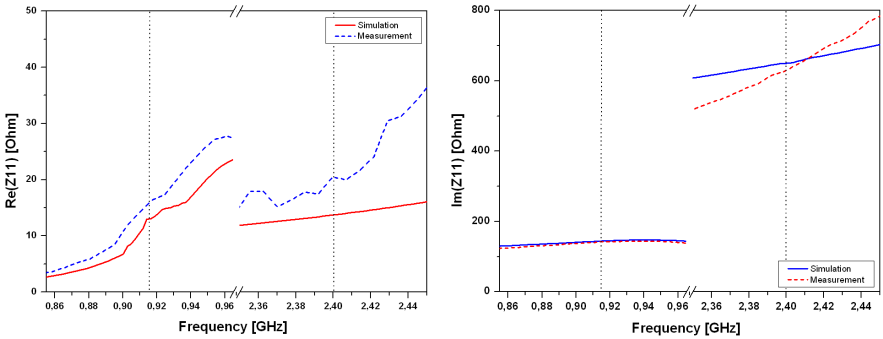

Figure 5. Measured and simulated input impedances of the antenna.

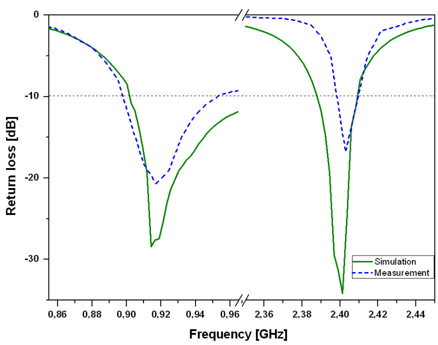

Figure 6. Measured and simulated power reflexion coefficients.

which allows a good match to the chip. As shown in the figure, the agreement between the simulated and measured reflexion coefficients is fairly good, and the discrepancy can be attributed to fabrication tolerance and calibration error.

4.2. Power Reflection Coefficient

The measured and simulated power reflection coefficients are shown in Figure 6. From the figure, we observe that the power reflection coefficient is roughly −20 dB @ 915 MHz, with an operating bandwidth of 50 MHz on a −10 dB level, and −17 dB @ 2.4 GHz with a bandwidth of 14 MHz.

4.3. Radiation Pattern

The simulated antenna's radiation patterns (E&H plan), at 915 MHz and 2.4 GHz, are shown in Figure 7. The radiation patterns are omnidirectional on the first band and nearly and also at the high band. The simulated peak gain is about 1.11 dBi @ 915 MHz and 1.15 dBi @ 2.4 GHz.

4.4. Read Range

A comparison between theoretically and experimentally estimated read ranges is illustrated in Figure 8. Tag range was computed using formula (2), simulated and measured values for the power reflection

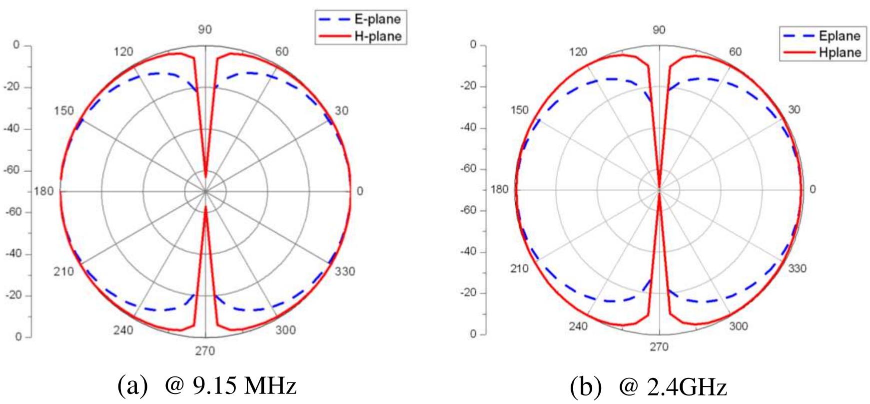

Figure 7. Radiation pattern of the antenna.

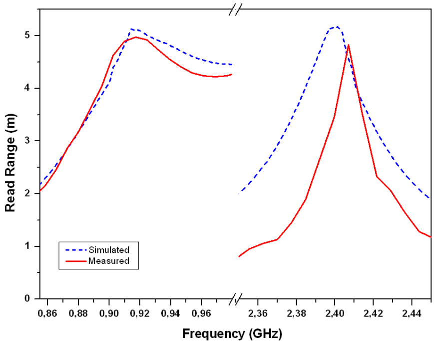

Figure 8. Estimated tag read range.

coefficient and tag antenna gain, considering the standardized EIRP = 4 W for the reader and the threshold power of the chip which is $P_{th} = -10\,\text{dBm}$.

From the result, it can be seen that theoretical and experimental curves are in close agreement, and the tag presents a reading distance of about 5 m @ 915 MHz band, and 4.5 @ 2.4 GHz.

5. CONCLUSION

A new dual band RFID dipole antenna has been proposed and experimentally demonstrated. Dual band and size reduction are achieved by using third iteration tree fractal shape. The Kurokawa's method and Friis free-space formula have been applied to calculate the theoretical power reflexion coefficient and the maximum readable range, respectively. The simulated and measured results demonstrate good agreement. This type of dual band antenna can be used in different kinds of small RFID readers, wireless sensor network nodes and other compact wireless systems.

REFERENCES

1. Ahson, S. and M. Ilyas, *RFID Handbook: Applications, Technology, Security, and Privacy*, CRC Press, Taylor & Francis Group, 2008.
2. Iliev, P., P. Le Thuc, C. Lucey, and R. Staraj, "Dual band HF-UHF RFID tag antenna," *Electronics Letters*, Vol. 45, No. 9, April 2009.
3. Kuo, J.-S, J. J. Wang, and C. Y. Huang, "Dual frequency for RFID tag with complementary characteristics," *Microw. Opt. Technol. Let.*, Vol. 49, No. 6, 1396–1397, 2007.
4. Fang, Z., R. Jin, and J. Geng, "Dual-band RFID transponder antenna design for specific chip without additional impedance matching network," *Microw. Opt. Technol. Let.*, Vol. 50, No. 1, 58–59, 2008.
5. Lee, Y.-C. and J.-S. Sun, "Dual-band dipole antenna for RFID tag applications," *Proc. 38th Euro. Microw. Conf.*, Amsterdam, Oct. 2008.
6. Jon, S., Y. Yu, and J. Choi, "Dual-band slot-coupled dipole antenna for 900 MHz and 2.45 GHz RFID tag application," *Electronics Letters*, Vol. 42, No. 22, 1259–1260, Oct. 2006.
7. Mandelbrot, B., *The Fractal Geometry of Nature*, WH Freeman and Co., 1977.

8. Werner, D. H. and S. Ganguly, "An overview of fractal antenna engineering research," *Ant. Prop. Mag.*, Vol. 45, No. 1, 38–57, 2003.
9. Puente, C., J. Romeu, R. Pous, X. Garcia, and F. Benitez, "Fractal multiband antennas based on the Sierpinski gasket," *Electronics Letters*, Vol. 32, No. 1, Jan. 1996.
10. Puente, C., J. Romeu, and A. Cardama, "The Koch monopole: A small fractal antenna," *IEEE Trans. Antennas Propag.*, Vol. 48, No. 11, Nov. 2000.
11. Puente, C., J. Claret, F. Sagues, J. Romeu, M. Q. Lopez-Salvans, and R. Pous, "Multiband properties of a fractal tree antenna generated by electrochemical decomposition," *Electronics Letters*, Vol. 32, No. 25, 2298–2299, 1996.
12. Werner, D. H., A. R. Bretones, and B. R. Long, "Radiation characteristics of thin-wire ternary fractal trees," *Electronics Letters*, Vol. 35, No. 8, 609–610, 1996.
13. Spence, T. G. and D. H. Werner, "A novel miniature broadband/multiband antenna based on an end-loaded planar open-sleeve dipole," *IEEE Trans. Antennas Propag.*, Vol. 54, No. 12, 3614–3620, 2006.
14. Nikitin, P. V., S. Rao, K. V. Lam, V. Pillai, R. Martinez, and H. Heinrich, "Power reflexion coefficient analysis for complex impedances in RFID tag design," *IEEE Trans. Microw. Theo. Tech.*, Vol. 53, No. 9, 2721–2725, Sep. 2005.

射 频 和 天 线 设 计 培 训 课 程 推 荐

易迪拓培训(www.edatop.com)由数名来自于研发第一线的资深工程师发起成立，致力并专注于微波、射频、天线设计研发人才的培养；我们于 2006 年整合合并微波 EDA 网(www.mweda.com)，现已发展成为国内最大的微波射频和天线设计人才培养基地，成功推出多套微波射频以及天线设计经典培训课程和 ADS、HFSS 等专业软件使用培训课程，广受客户好评；并先后与人民邮电出版社、电子工业出版社合作出版了多本专业图书，帮助数万名工程师提升了专业技术能力。客户遍布中兴通讯、研通高频、埃威航电、国人通信等多家国内知名公司，以及台湾工业技术研究院、永业科技、全一电子等多家台湾地区企业。

易迪拓培训课程列表：http://www.edatop.com/peixun/rfe/129.html

射频工程师养成培训课程套装

该套装精选了射频专业基础培训课程、射频仿真设计培训课程和射频电路测量培训课程三个类别共 30 门视频培训课程和 3 本图书教材；旨在引领学员全面学习一个射频工程师需要熟悉、理解和掌握的专业知识和研发设计能力。通过套装的学习，能够让学员完全达到和胜任一个合格的射频工程师的要求…

课程网址：http://www.edatop.com/peixun/rfe/110.html

ADS 学习培训课程套装

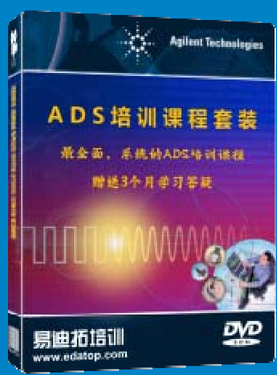

该套装是迄今国内最全面、最权威的 ADS 培训教程，共包含 10 门 ADS 学习培训课程。课程是由具有多年 ADS 使用经验的微波射频与通信系统设计领域资深专家讲解，并多结合设计实例，由浅入深、详细而又全面地讲解了 ADS 在微波射频电路设计、通信系统设计和电磁仿真设计方面的内容。能让您在最短的时间内学会使用 ADS，迅速提升个人技术能力，把 ADS 真正应用到实际研发工作中去，成为 ADS 设计专家...

课程网址： http://www.edatop.com/peixun/ads/13.html

HFSS 学习培训课程套装

该套课程套装包含了本站全部 HFSS 培训课程，是迄今国内最全面、最专业的 HFSS 培训教程套装，可以帮助您从零开始，全面深入学习 HFSS 的各项功能和在多个方面的工程应用。购买套装，更可超值赠送 3 个月免费学习答疑，随时解答您学习过程中遇到的棘手问题，让您的 HFSS 学习更加轻松顺畅…

课程网址：http://www.edatop.com/peixun/hfss/11.html

CST 学习培训课程套装

该培训套装由易迪拓培训联合微波 EDA 网共同推出，是最全面、系统、专业的 CST 微波工作室培训课程套装，所有课程都由经验丰富的专家授课，视频教学，可以帮助您从零开始，全面系统地学习 CST 微波工作的各项功能及其在微波射频、天线设计等领域的设计应用。且购买该套装，还可超值赠送 3 个月免费学习答疑…

课程网址：http://www.edatop.com/peixun/cst/24.html

HFSS 天线设计培训课程套装

套装包含 6 门视频课程和 1 本图书，课程从基础讲起，内容由浅入深，理论介绍和实际操作讲解相结合，全面系统的讲解了 HFSS 天线设计的全过程。是国内最全面、最专业的 HFSS 天线设计课程，可以帮助您快速学习掌握如何使用 HFSS 设计天线，让天线设计不再难…

课程网址：http://www.edatop.com/peixun/hfss/122.html

13.56MHz NFC/RFID 线圈天线设计培训课程套装

套装包含 4 门视频培训课程，培训将 13.56MHz 线圈天线设计原理和仿真设计实践相结合，全面系统地讲解了 13.56MHz 线圈天线的工作原理、设计方法、设计考量以及使用 HFSS 和 CST 仿真分析线圈天线的具体操作，同时还介绍了 13.56MHz 线圈天线匹配电路的设计和调试。通过该套课程的学习，可以帮助您快速学习掌握 13.56MHz 线圈天线及其匹配电路的原理、设计和调试…

详情浏览：http://www.edatop.com/peixun/antenna/116.html

我们的课程优势：

※ 成立于 2004 年，10 多年丰富的行业经验，

※ 一直致力并专注于微波射频和天线设计工程师的培养，更了解该行业对人才的要求

※ 经验丰富的一线资深工程师讲授，结合实际工程案例，直观、实用、易学

联系我们：

※ 易迪拓培训官网：http://www.edatop.com

※ 微波 EDA 网：http://www.mweda.com

※ 官方淘宝店：http://shop36920890.taobao.com